

Neutron spectroscopy of phonons in stage-1 rubidium-intercalated graphite

W. A. Kamitakahara

*Kernforschungszentrum Karlsruhe, Institut für Angewandte Kernphysik I, Postfach 3640, D-7500 Karlsruhe 1,
Federal Republic of Germany
and Ames Laboratory* and Department of Physics, Iowa State University, Ames, Iowa 50011*

N. Wada[†]

Coordinated Science Laboratory and Materials Research Laboratory, University of Illinois at Urbana—Champaign, Urbana, Illinois 61801

S. A. Solin

Department of Physics, Michigan State University, East Lansing, Michigan 48824

L. M. Seaverson

Ames Laboratory and Department of Chemistry, Iowa State University, Ames, Iowa, 50011

(Received 23 November 1982)

Neutron scattering measurements have been carried out on the graphite intercalation compound RbC_8 . Phonon dispersion curves were measured for *c*-axis longitudinal modes and for some transverse branches with wave vectors in the basal plane and polarization out of plane. For the latter, there is a strong deviation of the dispersion relation from that of pure graphite. In addition, a partial phonon density of states was determined for intercalate (Rb) vibrations by in-basal-plane inelastic scattering. Our analysis shows that a two-dimensional (2D) Born–von Kármán model with nearest-neighbor Rb-Rb force constants cannot account for the intercalate mode spectrum. A three-dimensional model in which the Rb-Rb forces are due to an unscreened Coulomb interaction agrees well with the data, implying that conduction-electron screening of the Rb-ion motions is substantially reduced in RbC_8 relative to Rb metal.

I. INTRODUCTION

The highly unusual structural and electronic characteristics^{1–3} of graphite intercalation compounds manifest themselves strongly in the physical properties of these materials, and the phonon properties are no exception. In the present paper we report a study on the lattice dynamics of the compound RbC_8 by inelastic neutron scattering. In general, most of the vibrational modes in such a solid can be described as graphite derived or intercalate derived. Since the Rb atoms are relatively massive and weakly bound, most of the low-frequency motions are alkali-metal-like. However, because of the weak interlayer binding, some low-frequency graphitelike motions also exist, and for some modes there is a strong coupling or hybridization between the Rb-like and C-like motions. The distinguishing feature of this coupled motion is that out-of-plane atomic displacements are involved, thus bringing the weakness of the interlayer forces into play. The [001]L (longitudinal) rigid-layer modes, and the transverse modes with \vec{q} vectors in the plane, but displacements out of plane (hereafter denoted [100] T_1 , or simply T_1), represent the basic motions of this type, other similar modes being describable as combinations of these two kinds of phonons. The [001]L modes of alkali-metal graphite intercalation compounds (AGIC's) have been extensively studied by Zabel and Magerl.⁴ The [100] T_1 modes, on the other

hand, have not been investigated in detail up to now, our present study on such modes being one of the first of its kind. In contrast to T_1 modes, for phonons involving in-layer displacements, the motions of alkali-metal and carbon atoms are generally decoupled, mainly because of the much stronger in-plane forces between C atoms. For the alkali-metal-like in-plane modes, we have been able to measure⁵ a partial phonon density of states which comprises those alkali-metal-like modes with both phonon wave vector and displacements parallel to the basal plane.

The primary goals of the present investigations are (i) to obtain a comprehensive picture of the low-frequency phonon spectrum of RbC_8 and (ii) to obtain information about the metal-metal and metal-carbon interactions which determine this picture in RbC_8 and the many related AGIC's. A noteworthy feature² of this class of compounds is the occurrence of order-disorder phase transformations within the intercalate substructure. The exact nature of the ordered and disordered phases has been the subject of some controversy. One point of view⁶ is that the intercalate in the disordered phase is liquidlike above the transformation temperature, and solidlike below it. The transformation itself is thus regarded as a kind of sublattice melting, perhaps quasi-two-dimensional in nature for high-stage materials. Knowledge concerning the nature and magnitude of the *M*-C (metal-carbon) and C-C interactions should be of value in forming a more accurate

Our convention does not correspond to the primitive unit cell,⁹ which is defined by entirely nonorthogonal vectors $\vec{t}_1=(0,2a,0)$, $\vec{t}_2=(-\sqrt{3}a,a,0)$, and $\vec{t}_3=(-(\sqrt{3}/2)a, -a/2,2I_c)$. However, our choice is more convenient experimentally and for purpose of comparison with other phonon data.

The neutron scattering measurements were carried out mostly on a triple-axis spectrometer operated by Ames Laboratory at the Oak Ridge Research Reactor, ORNL. Some data were taken on a triple-axis spectrometer at the High Flux Isotope Reactor, ORNL. In both cases, the (002) planes of graphite were used as monochromator and analyzer. A fixed scattered neutron energy $E_F=3.3$ THz=13.6 meV was used throughout, with pyrolytic graphite filters between sample and analyzer to eliminate order contamination. Constant- Q scans were always used for the phonon measurements. Most of the measurements were made with the sample still in its glass intercalation vessel.

III. RESULTS: PHONON DISPERSION

A neutron scattering study on RbC₈ has previously been reported by Ellenson *et al.*,¹⁵ who studied (i) [001]L phonon dispersion and (ii) the c -axis stacking order of the Rb layers at two temperatures, approximately 290 and 730 K. In the present investigation we performed measurements only at temperatures $T < 295$ K, and concentrated on aspects of the lattice dynamics not previously explored, i.e., intercalate modes and [100]T₁ modes. We also repeated the [001]L room-temperature phonon dispersion measurements, since these phonons could be measured conveniently and rapidly. The frequencies are generally in good agreement with Ref. 15; the only perceptible difference occurs for the modes near 3.5 THz at the Γ point in Fig. 2, where instead of the broad distribution reported in Ref. 15, we observed only a single, relatively sharp peak. The [001]L data for RbC₈ can be fitted rather well with a first-nearest neighbor, one-dimensional Born-von Kármán model, regarding the planes along the c axis as a linear diatomic chain. The fit is not quite as good as in the case of pure graphite,¹⁸ where a similar model fits the data within experimental error. Departures for our model are small ($\Delta v/v \sim 0.03$) but significant. From our data alone, one might conclude that first-nearest-neighbor interplanar forces strongly predominate, with small but non-negligible forces to more distant planes. It might be noted, however, that when compared with the extensive data of Zabel and Magerl⁴ for the [001]L phonon dispersion in many AGIC's, RbC₈ stands out as the only case where such a simple picture accurately accounts for experiment. This is somewhat incongruous, since the similarity of RbC₈, KC₈, and CsC₈ suggests that the physics underlying the lattice dynamics should be much the same in the three cases. The possibility exists that the apparent predominance of nearest-neighbor interplanar forces in the RbC₈ case is an artifact of oversimplified analysis.

On the left-hand side of Fig. 2, the [001]L dispersion relation is plotted in a manner corresponding to the actual dimensions of the Brillouin zone produced by $\alpha\beta\gamma\delta$ stacking.

cent layers (two Rb and two C layers), there are four branches to the [001]L dispersion relation. The convention used here differs from that adopted in Refs. 4 and 15, where a single graphite-alkali-metal bilayer is considered as a unit cell, giving rise to only two branches. Our four branches are, of course, merely these two branches folded once along c^* .

The [001]L dispersion relation comprises the only phonon branches which can be measured entirely without ambiguity,¹⁸ if a pyrolytic-graphite-based sample is used. For these and only these modes, the neutron wave-vector transfer is directed along the common aligned c axis of the crystallites, and one can use the identical method applicable to single-crystal samples. Substantially more information can be obtained with an only moderately increased degree of ambiguity, if the characteristics of graphite are taken into account, viz., the strongly layered nature of graphite and elastic isotropy in the basal plane. The possibilities were extensively explored in the case of pure graphite by Nicklow *et al.*¹⁹ In the present investigation we attempt a similar exploration for RbC₈, focusing on those aspects which differentiate the intercalation compound from pure graphite.

As shown by Nicklow *et al.*¹⁹ for the case of pure graphite, even with a pyrolytic graphite (PG) sample, it is possible to measure the TA₁ and TO₁ phonon energies as sharp peaks in the neutron spectra because of the near isotropy of the dispersion relation in the basal plane. The results of analogous measurements on our PG-based RbC₈ sample are displayed on the right-hand side of Fig. 2. Typical wave-vector transfers \vec{Q} employed in the constant- \vec{Q} scans are indicated as B1 and B2 in Fig. 3. The middle branches in Fig. 2 were measured along B2, whereas the highest and lowest-frequency branches were measured along B1. We stress that even though we designate these branches as [100]T₁ for the sake of convenience, these are dispersion relations averaged over all directions in the basal plane. For pure graphite, Nicklow *et al.*¹⁹ found it possible to trace such average dispersion curves to the Brillouin-zone boundary at $\xi=0.5(4\pi/\sqrt{3}a)$. For RbC₈, we found that measurements up to $q_m=0.25(4\pi/\sqrt{3}a)$ were feasible, corresponding to the zone

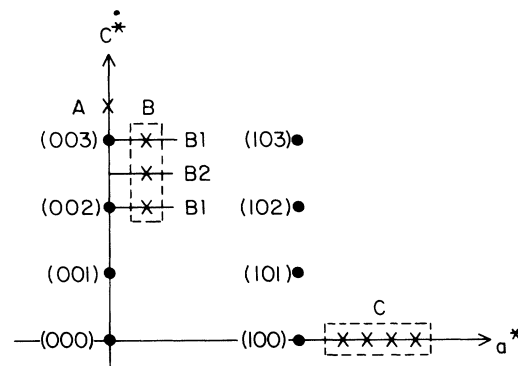


FIG. 3. The \times 's indicate Q vectors used to measure [001]L modes (A), [100]T₁ modes (B), and intercalate modes (C).

boundary of a 2×2 Rb layer. Probably, graphitelike modes can be observed at even larger wave vectors $q \gg q_m$, but reliable data on the coupled Rb-graphite motion were found to be restricted to $q \leq q_m$. The TA_1 branch is very different from pure PG, as shown in Fig. 2. In pure graphite the T_1 phonons are essentially intraplanar modes, with energies determined mainly by the strong in-plane bonding of the carbon nets. Since it is unlikely that the C—C bonding is very different in RbC_8 , large vibrational amplitudes for the Rb atoms at these low frequencies are implied. Qualitatively, the situation is reminiscent of low-frequency resonant modes of heavy atoms in a matrix of lighter atoms, where strong perturbation of the host lattice frequencies occurs mostly at low frequencies and is largest at some fairly well-defined resonant frequency. The analogous frequency for out-of-plane vibrations of Rb in RbC_8 would be about 3 THz. This corresponds to the $[001]L$, $\xi=0.5$ zone-boundary frequency, in which only the Rb atoms move, alternate Rb layers vibrating 180° out of phase against each other. From another point of view, the deviation from graphite tends to be largest at wave vectors near the new zone boundary due to the 2×2 superlattice formed in each Rb layer. Thus the degree of coupling for Rb and C out-of-plane motions should be greatest near a frequency of 3 THz and a wave vector $q_{xy} \simeq q_m$, as suggested by the appearance of our experimental dispersion curves for RbC_8 .

Perhaps the most interesting feature of the $[100]TA_1$ mode in graphite is the tendency for $\omega \sim q^2$ behavior at low q , i.e., a parabolic rather than a linear dispersion relation. An isolated thin sheet of homogeneous matter would indeed have such a dispersion curve for T_1 modes.^{20,21} Graphite represents the closest realization¹⁹ in the solid state to such behavior, which is also apparent to a lesser extent in MoS_2 and other layered compounds.^{22,23} The effect of interlayer coupling is to produce a finite slope as $q \rightarrow 0$, so that the small- q dispersion relation has the form $\omega^2 = aq^2 + bq^4$, where a and b arise from interlayer and intralayer force constants, respectively. The slope of the dispersion curve as $q \rightarrow 0$, i.e., \sqrt{a} , is a measure of $(C_{44}/\rho)^{1/2}$, where C_{44} is the elastic constant related to a shearing motion of rigid parallel layers. The $q \rightarrow 0$ slope of the $[100]TA_1$ branch is the same as that of the $[001]TA$ branch. This leads to the possibility of measuring C_{44} by neutron scattering. Ultrasonic methods have so far had a very limited application²⁴ to AGIC's from which, to our knowledge, no estimate of C_{44} have been made. Very recently, estimates of the shearing elastic constant have been made for RbC_{44} , KC_8 , KC_{24} , and CsC_8 by Zabel *et al.*²⁵ through analysis of neutron scattering measurements in which HOPG-based samples with $2-3^\circ$ mosaic spread were used. Unfortunately, the 6° mosaic spread of our RbC_8 sample is somewhat too large to permit a reliable estimate of C_{44} at present. In the AGIC's studied by Zabel *et al.* it was found that C_{44} was much softer in RbC_{24} and KC_{24} than in pure graphite, by at least a factor of 4 or 5. A smaller but still substantial softening is present for the stage-1 compounds CsC_8 and KC_8 . Thus it is likely that C_{44} is also somewhat smaller in RbC_8 than in graphite.

Lattice dynamical models for graphite intercalation

compounds have recently been formulated by Leung *et al.*,²⁶ Al-Jishi and Dresselhaus,¹⁰ and by Horie *et al.*⁹ The calculations of Horie *et al.* for KC_8 and RbC_8 employed a Born—von Kármán model with ten force constants, of which six are related to the intralayer forces in pure graphite and are likely to be very reliable for the purpose at hand. Two others are related to the C—K interlayer interactions, and the last two to K—K intralayer forces. The former were fitted to the $[001]L$ neutron scattering data of Ellenson *et al.*¹⁵ on RbC_8 and assumed to be the same for KC_8 , whereas the latter were identified with force constants in pure-K metal, in the absence of other information. The calculation of Horie *et al.* accounts qualitatively for some Raman scattering observations on the perturbation of graphite-derived modes. The calculated frequencies for the low-frequency zone-center modes polarized parallel to c^* lie somewhat higher than the neutron measurements. For B_{1g} and B_{1u} modes, the calculation gives 6.09 and 7.26 THz for KC_8 , and 4.89 and 6.78 THz for RbC_8 , whereas the corresponding neutron-measured values are 5.08, 5.98, 3.50, and 4.66 THz, respectively. It thus appears that the carbon—alkali-metal interlayer force constant should be decreased somewhat in the calculation. Also, the alkali-metal—alkali-metal in-layer force constants should be increased substantially, in view of our data on intercalate modes described below. Undoubtedly, if these simple numerical adjustments were made, much better agreement with neutron experiments (Refs. 15 and 4 and the present study) would be obtained.

Whereas Ref. 9 represents a relatively simple calculation for two specific stage-1 compounds with the same crystal structure, the calculations of Al-Jishi and Dresselhaus¹⁰ (AD) constitute a more ambitious effort to account for a wide variety of data on the lattice modes of many AGIC's, including higher-stage compounds with complicated and/or disordered structures. These calculations achieve a great deal of success in describing Raman scattering, sound velocity, $[001]L$ neutron, and specific-heat measurements. In order to avoid the difficulty of considering the ill-defined or unknown in-plane structures of some AGIC's, AD assumed that each unit cell of a stage- n compound contained only one intercalate atom and $2n$ carbon atoms. For modes which are mainly graphite derived, or for those in which the intercalate layers move as rigid units (i.e., low-frequency $[001]L$ and $[001]T$ branches), this assumption allows a convenient, accurate, and fruitful approach to the lattice dynamics of AGIC's. Its consequences for modes in which the intercalate substructure may be more important (e.g., $[100]T_1$ and intercalate modes) have yet to be determined, but there is good agreement with neutron data²⁵ on RbC_{24} . Since the calculations were made without taking the most recent neutron data into account, it is not surprising that there are at present some points of discrepancy between the AD calculations and experiment. Like the model of Horie *et al.*, however, some attempt to adjust model parameters needs to be made before a definitive comparison with experiment is possible. Also, comparison of the Horie and AD models with similar force-constant parameters should shed light on the question of the effect of intercalate substructure on phonon dispersion.

IV. INTERCALATE MODES

In contrast to the out-of-plane modes, which generally reflect strongly-coupled Rb-C motions at low frequencies, the in-plane motions of RbC₈ are largely decoupled, because of the very great difference between in-plane C-C and Rb-Rb forces. Of course, there must be a region of small q and ω wherein the acoustic mode character is such that C and Rb atoms move in phase. However, for in-plane motion, this region is rather small, with $q_{xy} \leq 0.03$ ($4\pi/\sqrt{3}a$), and the large majority of in-plane modes can be regarded as almost purely graphitelike or Rb-like. As described in a previous publication,⁵ the method for measuring these modes is to direct the wave-vector transfer \vec{Q} in the basal plane, and to make constant- $|\vec{Q}|$ scans for a number of values of $|\vec{Q}|$ to obtain a good averaging over the in-plane intercalate phonon density of states. This method is essentially the same²⁷⁻²⁹ as that used to determine the phonon density of states of three-dimensional (3D) polycrystals, except that in the case of PG-based RbC₈, we are dealing with a two-dimensional (2D) polycrystal, i.e., one with random crystallite orientations only within a plane. The phonon density of states that we thus determine is a partial phonon density of states in the sense that only phonons with wave vectors and atomic displacements in the basal plane are represented. The method is also rather similar to that used by Taub *et al.*³⁰ to study the dynamics of Ar monolayers adsorbed on the c surface of graphite, except that the PG-based material used here is much more highly oriented than the exfoliated Grafoil material used in the adsorbate investigations. The low incident energy and lack of high orientation did not permit the determination of a phonon density of states for Ar monolayers on Grafoil. However, by comparing their data with appropriate calculations for a 2D Born-von Kármán model, Taub *et al.* showed that the phonons were like those of a 2D solid with force constants determined by the same Lennard-Jones pair interaction as in Ar gas. Out-of-plane dynamics were dominated by a resonant mode of the heavy Ar atoms, a situation reminiscent of out-of-plane modes in RbC₈, as described in Sec. III.

The experimental method of in-plane scattering used here implicitly tends to regard the intercalate layers as 2D solids, in that we do not look at modes with wave vectors \vec{q} with out-of-plane components. That is, the partial phonon density of states (PDOS) that we determine is not simply the eigenvector-projected PDOS, which would be, using \vec{e} for phonon eigenvectors, a 3D Brillouin-zone sum

$$g_{xy}(\nu) = \sum_{jq_x q_y q_z} [e_x^2(\text{Rb}, j) + e_y^2(\text{Rb}, j)] \delta(\nu - \nu_j). \quad (1)$$

Rather we measure $g'_{xy}(\nu)$, a similar but not identical function which excludes the sum over q_z , setting $q_z = 0$. For the case of completely rigid graphite layers and no force constants connecting neighboring Rb layers, the two functions would be the same. In practice, since $g'_{xy}(\nu)$ is a set of zero measure, some relaxation of the restriction $q_z = 0$ is necessary in order to obtain a finite neutron scattering cross section. Thus the function we obtain includes modes with q_z lying between limits $\pm q_z^{\max}$ determined by instru-

mental q resolution, and more importantly, by the mosaic spread of the sample. The out-of-plane angular acceptance due to these factors is about $\pm 3^\circ$, implying $q_z^{\max} \simeq 0.07 \text{ \AA}^{-1}$. Since this is much less than $(2\pi/I_c) = 1.1 \text{ \AA}^{-1}$, the wave vector characterizing the correlated motion of nearest-neighbor Rb planes, the function we determine is an accurate representation of $g'_{xy}(\nu)$.

Several scans with $4.0 < Q < 4.7 \text{ \AA}^{-1}$ were made, and the sum was used to obtain the PDOS shown in Fig. 4. At these low phonon energies, there is very little response from the graphite layers, as shown experimentally by a similar scan on pure pyrolytic graphite, which gave only a gently sloping, featureless spectrum which was subtracted as background from the RbC₈ spectrum. Dividing the background-corrected spectrum by the factor $\{\exp(\beta h \nu)^{-1} + 1\}/\nu$ in the one-phonon neutron scattering cross section yields the PDOS in Fig. 4. The non-response of graphite is to be expected from the very strong forces opposing in-layer C displacements within a graphite layer. The dispersion curves for pure graphite¹⁹ show that no graphite phonons below 4-THz energy can be excited with in-plane scattering geometry except within a distance in reciprocal space of 0.1 \AA^{-1} to a graphite Bragg ring. Such rings were explicitly avoided in choosing Q values for the scans. The distance of closest approach to a ring was 0.4 \AA^{-1} . Hence no graphite response was expected, nor observed.

The general appearance of the PDOS is roughly what one might expect for a 2D solid comprising an individual intercalate layer, the lower- and higher-frequency peaks, of roughly equal weight, being the in-plane transverse and longitudinal components of the PDOS. However, the simplest analysis that can be made by regarding each Rb layer as a 2D solid does not permit an adequate fit to experiment. Assuming a 2D Born-von Kármán model for a triangular lattice with nearest-neighbor (NN) radial force constants α yields the PDOS shown in Fig. 5. The transverse peak is too high in energy, and when resolution is folded in the minimum between the peaks is too shallow. Even if a second parameter ν_0 , representing the C-Rb interaction, is introduced, the best fit (Fig. 4) is not in good

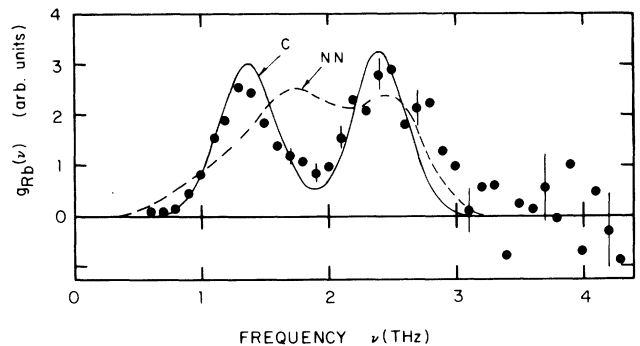


FIG. 4. In-plane partial phonon density of states for intercalate modes in RbC₈ at room temperature, compared with 2D Born-von Kármán model (NN) and Coulomb force model (C). Both model spectra have been broadened with a Gaussian of 0.5 THz FWHM to account for resolution and anharmonicity.

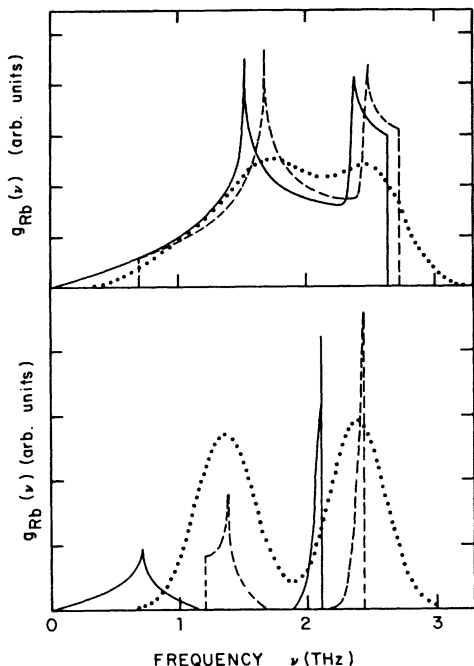


FIG. 5. Top: phonon density of states for a 2D Born–von Kármán model (—), including interaction with graphite (---), and broadening due to resolution and anharmonicity (···). Bottom: similar curves for Coulomb force model.

agreement with experiment. The parameter ν_0 has a simple interpretation. It is the frequency for in-plane vibrations of an Rb atom when the Rb-Rb interactions are turned off. It hence represents the curvature at the bottoms of the depressions in the potential surface for an Rb atom due to the bounding carbon layers. A lower cutoff is created at ν_0 , suppressing the $g(\nu) \sim \nu$ low- ν behavior of the 2D solid. This improves agreement with experiment at low ν but worsens it at higher ν , squeezing the transverse peak further toward the longitudinal peak. The effects of ν_0 and instrumental resolution on the PDOS are shown in Fig. 5 (top).

The inadequacy of the 2D Born–von Kármán model implies that longer-range forces need to be included. An improved fit could certainly be obtained by introducing more adjustable parameters to represent these forces, but the validity of such a fit in the absence of more detailed information (phonon dispersion rather than just a PDOS) is questionable. In the following we show that a long-range 3D force model can be constructed without introducing more adjustable parameters, and with a well-defined physical interpretation. We identify three contributions to the dynamical matrix of the Rb sublattice. First, there is the Coulomb interaction between Rb^+ ion cores, in a uniform neutralizing negative background, giving a contribution which can be computed to infinite range by the standard method of Ewald summation.³¹ Although the background is usually assumed to be three-dimensionally uniform in such a calculation, since the modes in our PDOS involve only in-layer displacements,

we are actually only assuming that it is uniform in the a - b plane. Second, there is the C-Rb interaction, which we represent again by the single parameter ν_0 , simply adding $m_{\text{Rb}}\nu_0^2$ to the xx and yy components of the dynamical matrix. Third, the screening of the Rb-ion motions by the conduction electrons and by the polarization of the ion cores gives a contribution which depends on the details of the electronic structure and is consequently more difficult to calculate. In fact, for the lattice dynamics of most simple metals and transition metals, this screening contribution is considered to be the only nontrivial one, since the Coulomb part can be evaluated exactly. In our calculation we neglect this third contribution entirely and yet achieve good agreement with experiment.

The expressions used for the Ewald sum were those given by Cohen and Heine in Ref. 31. At each of 200 wave vectors \vec{q} in the basal plane within the irreducible zone, the summation was carried out over 124 reciprocal-lattice vectors and 124 real-space lattice vectors. Each frequency was weighted with $(e_x^2 + e_y^2)$ to project out only motions parallel to the basal plane. In order to simplify the calculation somewhat, an $\alpha\beta\gamma$ stacking order of the Rb layers was assumed, instead of the actual $\alpha\beta\gamma\delta$ ordering, reducing the structure of the Rb sublattice to a monatomic rhombohedral structure. Otherwise an Ewald summation for a diatomic lattice would be necessary. Since the stacking sequences only differ in the fourth-neighboring Rb planes, a negligible effect on the frequency distribution is expected. We note that the summation is fully three dimensional. The calculated partial PDOS functions, with and without the C-Rb interaction, are shown in Fig. 5. The lower-frequency peak is still the transverse, in-plane phonon peak of the Rb sublattice. Inclusion of the C-Rb interaction shifts its position from 0.7 THz to $(\nu_0^2 + 0.49)^{1/2} = 1.4$ THz, taking $\nu_0 = 1.2$ THz. Thus our only adjustable parameter ν_0 in this model has been used to fit the frequency of the transverse peak.

In the absence of the C-Rb interaction, the upper, longitudinal peak occurs very nearly at the ion plasma frequency $\nu_p = e/(\pi m_{\text{Rb}} V)^{1/2} = 2.10$ THz, where V is the volume per Rb ion, shifting to $(\nu_p^2 + \nu_0^2)^{1/2} = 2.42$ THz when the previously fitted value, $\nu_0 = 1.2$ THz, is taken. No additional fitting is involved here; the frequency of the upper peak and the deep minimum between peaks arise naturally from the calculation. The conclusion from the good agreement between this Coulomb force model and experiment is that conduction-electron screening is a much less important factor in determining the intercalate mode PDOS in RbC_8 than is usually the case for good metals. We do not mean to imply that the loss of screening is total, but only that its effect on most of the phonons is not large, so that the intercalate mode PDOS is not strongly modified. At long phonon wavelengths ($q \rightarrow 0$), the Coulomb contribution must be exactly canceled by the screening contribution, since the conduction electrons will readjust so as to nullify the nearly macroscopic electric fields arising from the ionic displacements. Strong effects due to screening are visualized as being confined to a region $q_{xy} < q_m$ in RbC_8 , where q_{xy} is the component of the phonon wave vector in the basal plane. The fraction of longitudinal phonons subject to screening is then approxi-

mately $r = (q_m/q_b)^2$, where q_b is a typical zone-boundary wave vector. Experiments on phonon dispersion in heavily doped semiconductors³² have demonstrated that in those materials $q_m \simeq 2k_F$. Although the details of the electronic structure^{33,34,3} of stage-1 AGIC's remain a subject of controversy, especially concerning the existence of an s-like alkali band, there is no doubt that any reasonable set of bands will generate some in-plane Fermi-surface calipers with $2k_F \sim q_b$; i.e., on this basis $r \sim 1$ and all longitudinal in-plane phonons should be affected by screening. In typical metallic elements and alloys, $2k_F \gg q_b$ and all longitudinal phonons are affected by screening to an extent that is dependent not merely on the dimensions of the Fermi surface, but mainly on the conduction-electron concentration, as shown in Table I. The effect of screening on the Rb motions in RbC₈ is apparently somewhat less than for pure Rb metal, which has the same conduction-electron—Rb-atom ratio. Most probably, this behavior arises because the conduction electrons now reside partially or wholly on the graphite layers, and furthermore the electronic structure is much more anisotropic than in Rb, both factors tending to limit the electronic response to ion displacement. Thus to some extent the lattice dynamics of RbC₈ are reminiscent of an ionic solid, even though it is a very good metal from the conductivity viewpoint.

V. SUMMARY

Detailed observations on the low-frequency lattice modes in RbC₈ have been carried out by neutron spectroscopy. The appearance of the phonon dispersion curves for layer "rippling"-type T₁ phonons implies a strong coupling between the graphite-layer motions and alkali motions. Graphite and intercalate are effectively decoupled in the case of the intercalate modes, which involve Rb motions parallel to the layers. The measured intercalate mode phonon density of states can be accurately accounted for by a simple 3D Coulomb-force model, in which conduction-electron screening of the ionic motion is neglected.

As for prospects for future experiments, it would be of interest to follow the phonon behavior as a function of temperature through the order-disorder phase transformation,^{15,2,6} which should occur at temperatures in the range

TABLE I. Number of conduction electrons per atom and ratio of maximum phonon frequency ν_p in simple metals and in RbC₈.

	Pb	Al	Na	RbC ₈
n_e	4	3	1	~ 1
ν_{\max}	0.20	0.30	0.53	~ 1
ν_p				

300–500 °C depending on the external vapor pressure.^{2,6} The transformation involves not only disordering, but also expulsion of some Rb from the sample to produce less-dense intercalate layers, and significant changes in the intercalate phonon properties should result.

Further analysis of the existing results in terms of a more comprehensive model, to account simultaneously for T₁ modes, intercalate modes and other known features of the vibrational spectrum, is desirable, but lies somewhat beyond the scope of the present article. Incorporation of neutron scattering data from this experiment on RbC₈, and similar data²⁵ on other AGIC's into models like those of Refs. 9 and 10 should be attempted. This should eventually lead to a definitive understanding of the lattice vibrational spectra of alkali-metal—graphite compounds.

ACKNOWLEDGMENTS

This work was supported primarily by the Office of Basic Energy Sciences, U.S. Department of Energy (U.S. DOE), and by the Kernforschungszentrum Karlsruhe. The Ames Laboratory is operated for the U.S. Department of Energy by Iowa State University under Contract No. W-7405-Eng-82 with the U.S. DOE. Other support was received by S. A. Solin from the U.S. Army Research Office (Grant No. DAA G-29-80-K-0003). It is a pleasure for one of us (W.A.K.) to thank W. Reichardt, F. G. Gompf, and L. Pintschovius of the Kernforschungszentrum Karlsruhe for their hospitality and advice during the author's stay at their institute. We also wish to acknowledge valuable discussions with H. Zabel of the University of Illinois.

*Permanent address.

† Present address: Schlumberger-Doll Research, P. O. Box 307, Ridgefield, CT 06887.

¹M. S. Dresselhaus and G. Dresselhaus, *Adv. Phys.* **30**, 139 (1981).

²S. A. Solin, *Adv. Chem. Phys.* **49**, 455 (1982).

³J. E. Fischer, *Mater. Sci. Eng.* **31**, 211 (1977).

⁴H. Zabel and A. Magerl, *Phys. Rev. B* **25**, 2461 (1982).

⁵W. A. Kamitakahara, N. Wada, and S. A. Solin, *Solid State Commun.* **44**, 297 (1982).

⁶R. Clarke, N. Caswell and S. A. Solin, *Phys. Rev. Lett.* **42**, 61 (1979); R. Clarke, N. Caswell, S. A. Solin, and P. M. Horn, *ibid.* **43**, 2018 (1979).

⁷U. Mizutani, T. Kondow, and T. B. Massalski, *Phys. Rev. B* **17**, 3165 (1978); M. Saganuma, T. Kondow, and U. Mizutani, *Phys. Rev. B* **23**, 706 (1981).

⁸M. G. Alexander, D. P. Goshorn, and D. G. Onn, *Phys. Rev. B* **22**, 4535 (1980).

⁹C. Horie, M. Maeda, and Y. Kuramoto, *Physica* **99B**, 430 (1980).

- ¹⁰R. Al-Jishi and G. Dresselhaus, *Phys. Rev. B* **26**, 4523 (1982).
- ¹¹L. Pietronero and S. Strässler, *Phys. Rev. B* **23**, 6793 (1981).
- ¹²A. Hérold, *Bull. Soc. Chim. Fr.* **187**, 999 (1955).
- ¹³D. E. Nixon and G. S. Parry, *J. Phys. D* **1**, 291 (1968).
- ¹⁴H. Zabel (private communication).
- ¹⁵W. B. Ellenson, D. Semmingsen, D. Guérard, D. G. Onn, and J. E. Fischer, *Mater. Sci. Eng.* **31**, 137 (1977).
- ¹⁶J. B. Hastings, W. B. Ellenson, and J. E. Fischer, *Phys. Rev. Lett.* **42**, 1552 (1979).
- ¹⁷G. S. Parry, *Mater. Sci. Eng.* **31**, 99 (1977), and references therein.
- ¹⁸G. Dolling and B. N. Brockhouse, *Phys. Rev.* **128**, 1120 (1962).
- ¹⁹R. M. Nicklow, N. Wakabayashi, and H. G. Smith, *Phys. Rev. B* **5**, 4951 (1972).
- ²⁰Lord Rayleigh, *Theory of Sound I* (MacMillan, London, 1894), Vol. 1, p. 352.
- ²¹K. Komatsu, *J. Phys. Soc. Jpn.* **10**, 346 (1955).
- ²²N. Wakabayashi, H. G. Smith, and R. M. Nicklow, *Phys. Rev. B* **12**, 659 (1975).
- ²³N. Wakabayashi, in *Electrons and Phonons in Layered Crystal Structures*, edited by T. J. Wieting and M. Schlüter (Riedel, Dordrecht, Holland, 1979), p. 409.
- ²⁴D. M. Hwang, B. F. O'Donnell, and A. Y. Wu, in *Physics in Intercalation Compounds*, Vol. 28 of *Springer Series in Solid State Sciences*, edited by L. Pietronero and E. Tosatti (Springer, New York, 1981).
- ²⁵H. Zabel, W. A. Kamitakahara, and R. M. Nicklow, *Phys. Rev. B* **26**, 5919 (1982).
- ²⁶S. Y. Leung, G. Dresselhaus, and M. S. Dresselhaus, *Phys. Rev. B* **24**, 6083 (1981).
- ²⁷B. P. Schweiss, B. Renker, E. Schneider, and W. Reichardt, in *Superconductivity in d- and f-Band Metals*, edited by D. H. Douglass (Plenum, New York, 1976), p. 189.
- ²⁸A. P. Roy and B. N. Brockhouse, *Can. J. Phys.* **48**, 1781 (1970).
- ²⁹M. M. Bredov, B. A. Kotov, N. M. Okuneva, V. S. Oskotskii, and A. L. Shakh-Bugadov, *Fiz. Tverd. Tela (Leningrad)* **9**, 287 (1967) [*Sov. Phys.—Solid State* **9**, 214 (1967)].
- ³⁰H. Taub, K. Carneiro, J. K. Kjems, L. Passell, and J. P. McTague, *Phys. Rev. B* **16**, 4551 (1977).
- ³¹R. A. Cowley, *Acta Crystallogr.* **15**, 687 (1962); M. L. Cohen and V. Heine, in *Solid State Physics*, edited by H. Ehrenreich, F. Seitz, and D. Turnbull (Academic, New York, 1970), Vol. 24, p. 114.
- ³²S. K. Sinha, *CRC Crit. Rev. Solid State Sci.* **3**, 273 (1973), and references cited therein.
- ³³T. Inoshita, K. Nakao, and M. Kamimura, *J. Phys. Soc. Jpn.* **43**, 1237 (1977); *ibid.* **45**, 689 (1978).
- ³⁴P. Oelhafen, P. Pfluger, E. Hauser, and H.-J. Güntherodt, *Solid State Commun.* **33**, 241 (1980).